

# GRANULOMETRIC MAPS FROM HIGH RESOLUTION SATELLITE IMAGES

CATHERINE MERING AND FRANCK CHOPIN

UMR CNRS PRODIG, Université Paris 7 Denis Diderot 2, place Jussieu, F 75252 Paris Cedex 05  
e-mail: mering@lgs.jussieu.fr; franckchopin@yahoo.fr  
(Accepted February 21, 2002)

## ABSTRACT

A new method of land cover mapping from satellite images using granulometric analysis is presented here. Discontinuous landscapes such as steppian bushes of semi arid regions and recently growing urban settlements are especially concerned by this study. Spatial organisations of the land cover are quantified by means of the size distribution analysis of the land cover units extracted from high resolution remotely sensed images. A granulometric map is built by automatic classification of every pixel of the image according to the granulometric density inside a sliding neighbourhood. Granulometric mapping brings some advantages over traditional thematic mapping by remote sensing by focusing on fine spatial events and small changes in one peculiar category of the landscape.

Keywords: high resolution images, mathematical morphology, texture classification.

## INTRODUCTION

The objective of the work presented here is to analyse discontinuous land covers from satellite images. Indeed, images of landscapes from high resolution remotely sensed views are relevant materials for the observation and quantification of some processes involved by artificial or natural action on the earth surface. The first process under study is urbanisation which leads to a progressive sealing of the soil surface by building up materials. It is quantified here from the image of the density of the built up areas which is extracted from the original Landsat TM sub scene. Another kind of dynamics analysed here is the contraction of ligneous cover in tropical lands during periods of acute dryness. The cinematic of the vegetation patchiness is quantified by comparing two SPOT scenes of a sahelian region, taken respectively after the dry and the wet season.

Thematic mapping from satellite images is classically performed by multispectral or multi-textural classification, textural parameters being computed from local or global statistics on grey-tone values of the image (Harralick, 1978). The objective here consists in analysing the spatial organisation of one single component of the landscape under study, such as built up surfaces or ligneous cover. The mapping of such component is obtained at the first step by processing the original scene with classical methods. Its spatial organisation is then analysed

through the size distribution of the particles from the binary image previously computed. For such a purpose, granulometric analysis on binary images (Matheron, 1975) is used here.

The final map is obtained by automatic classification of the pixels described by the values of granulometric densities inside a given neighbourhood of each pixel. This method provides a new kind of mapping by remote sensing, where segmentation of the image into landscape units depends only on the spatial organisation. Such maps are efficient tools to detect changes in the landscape that would not appear so clearly by multispectral or multitextural classical analysis (Mering *et al.*, 1997).

## MATERIAL AND METHODS

The granulometric mapping method from remote sensing images is described through the processing of a Landsat Thematic Mapper sub scene (may 1987) of the south-eastern part of Paris (France) and suburbs (Fig. 1). The image processing consists in three steps which are detailed in the following.

### EXTRACTION OF A SINGLE PHASE FROM MULTISPECTRAL SCENES

The component of the landscape is first extracted from the original multispectral scene to provide a binary image of the areas with the highest density of

built up areas. On the BGR coloured composition made with the two visible and the near infrared channels of the Landsat TM subscene (Fig. 1), buildings, roads, paths, and bare soils have very similar spectral signature, so that only spaces covered with vegetation (in red) and hydrographic net (in dark blue) may clearly be distinguished from built up areas (in cyan). In order to enhance the contrasts between the various objects of the scene, a Principal Component analysis (PCA) is first processed. The seven eigenvectors are provided here by applying the PCA algorithm to the correlation matrix computed from the seven channels of the Landsat TM sub scene and their co-ordinates are affected to the original values of all the pixels of the sub scene to form the PCA images. On the (BGR) coloured composition deduced from the first three ordered components of the P.C.A. (Fig. 2), the dense network of urban settlements inside Paris and the southern suburbs with intense activity as well as the hydrographic net (Seine and Marne rivers) appear in bright green and yellow, while residential and where area covered with vegetation appear in dark green, purple and red. After having extracted the hydrographic nets by a low threshold on TM4 channel, patterns corresponding to the highest density of constructions are then selected by means of a high threshold on the second component of the P.C.A. (Fig. 3) which was the green channel on the coloured composition image of (Fig. 2).

## GRANULOMETRIC ANALYSIS ON BINARY IMAGES

A binary image can be described as a set of the Euclidean space  $\mathbb{R}^2$ . Such a set consists in many subsets which are the connected components of the image. In order to assess the size distribution of the components of a set  $X$ , we use the method of granulometry by opening with a convex structuring element  $B(\lambda)$  with a size  $\lambda$  (Serra, 1982). The texture is quantified by computation of the granulometric density  $g_\lambda(X)$  which is defined as follows:

$$g_\lambda(X) = [A(XB(\lambda)) - A(XB(\lambda+1))] / A(X) \quad (1)$$

where  $A(X)$  is the measure of the set  $X$

Quantitative variables  $V_i$  used for classification of all the pixels  $P$  of the binary image are the following:

$$V_i(P) = g_i(F(P)) \quad (2)$$

where  $g_i(F(P))$  is the granulometric density computed at the step  $i$  of the opening sequence, inside the sliding measuring mask  $F(P)$  centred on pixel  $P$ .

$I$  is the size of  $B$  such that all the pixels of  $F(P)$  are eliminated after the *opening* by  $B_I$ . This value is computed for all sets  $F(P)$ . Each pixel of the image is then described by the  $I$  variables  $V_i$ .

## THE USE OF THE DANIELSSON DISTANCE

In order to optimise the computation of all the variables  $V_i$ , the distance of Danielsson (Danielsson, 1980; Borgefors, 1986) is first calculated on the original image from the binary image under study (Fig. 3). Successive erosions with a circular structuring element  $B$  of increasing size  $i$  are computed within one single step, by selecting the set of pixels with value superior to  $i$  on the distance image (Fig. 4). The computation of the successive openings needs an iterative computation of distance images from the previously eroded sets. The use of the distance of Danielsson still provides a substantial acceleration of the computation of granulometric densities around all the pixels of the image.

## MAPPING BY PIXELWISE CLASSIFICATION

The use of image processing software requires as input files images composed by pixels with integer values that must be stored within one single byte. For this reason, the values of  $V_i(P)$  which are basically positive decimal numbers inferior to 1 (see Eq. 1 and Eq. 2), are transformed into positive integer numbers comprised between 0 and 255 by a linear transformation.

All the pixels of resulting images are classified by the  $k$ -Means method (Diday, 1974). This method consists in finding  $k$  centres for the  $k$  classes which are computed by an iterative processing. At the first step  $k$  centres are randomly selected. Each following step consists in affecting pixels to the nearest centre according to the euclidian distance criterion and to recompute new centers from the  $k$  current clusters. According to the theorem of Huygens, the intra class variance tends to decrease as the interclass one tends to increase at each iteration of the processing. Final  $k$ -classes may then be interpreted according to the co-ordinates of their final respective centre, which correspond to the set of the mean values of each variable inside each class. In the case under study, each one of the  $k$  classes is then interpreted according to its mean granulometric density value  $v_i$ . The resulting image is a  $k$ -levels image, where each level determines a set of pixels belonging to the same class which is characterised by the value of  $v_i$ .

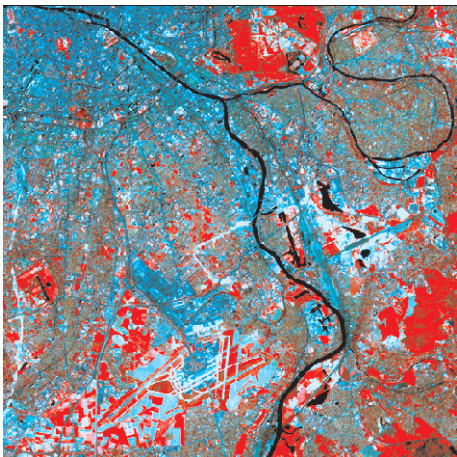


Fig. 1. Coloured composition from Landsat TM visible and infrared bands on the eastern part of Paris and suburbs.

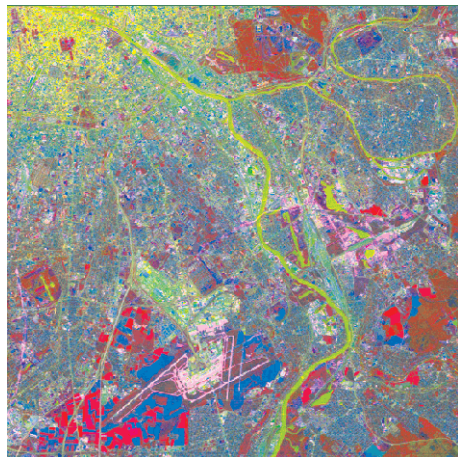


Fig. 2. Coloured composition from the first three PCA components computed from the seven Landsat TM channels.

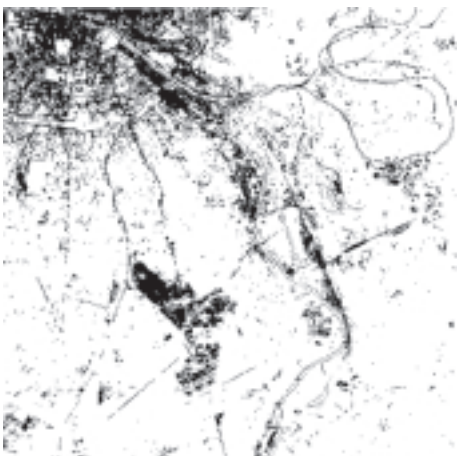


Fig 3. Extraction of areas having the higher density of constructions from a high threshold on the 2nd PCA component.

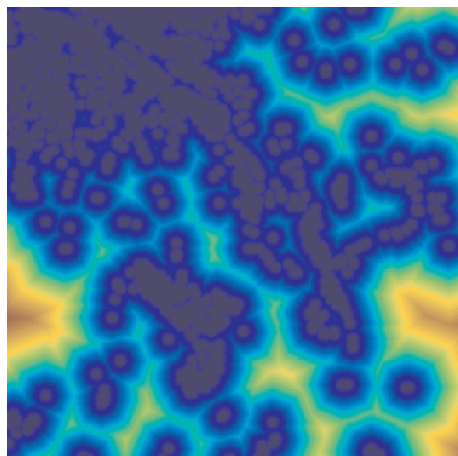


Fig. 4. The Danielsson distance image computed from image of Fig. 3.

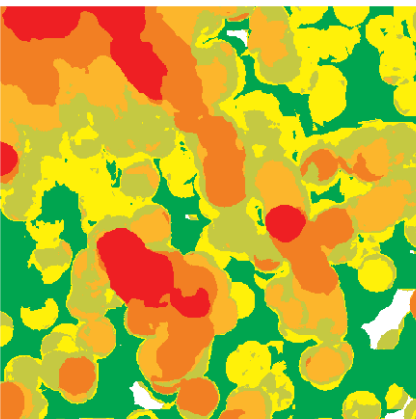


Fig. 5. Granulometric map of east of Paris with a 100 pixels-wide sliding mask.

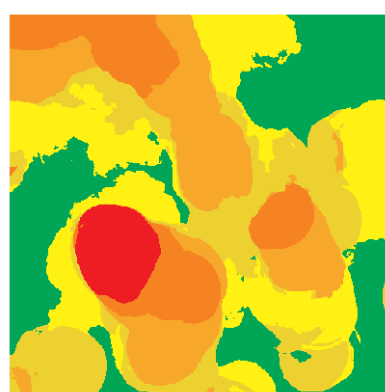


Fig. 6. Granulometric map of east of Paris with a 200 pixels-wide sliding mask.

A 6-Means classification is processed from the image of the areas having the highest density of constructions

in the east of Paris (Fig. 3). The mean granulometric density value  $v_i$  for each one of the 6 classes  $C_i$  is

given on Table 1. One can observe for instance from Table 1, that class 6 has a very high value for  $v_1$  and very low values for the others variables. It can be interpreted as containing especially small particles. The corresponding macro-texture is composed thence of small disconnected sets. At the opposite, class 1 is characterised by weak mean values for the first  $v_i$  variables and the highest values for the last ones. It is essentially composed of large particles. In this case, the non zero value appearing for the first granulometric values may be explained by the fact that the big particles are generally not convex and then a part of their surface is eliminated before the last steps of the opening sequence.

## RESULTS

Granulometric maps of the eastern part of Paris and suburbs obtained by the procedure previously described, with a 100 (resp. 200) pixels-wide sliding measuring mask from the initial Landsat TM of Paris (Fig. 1) are shown on Fig. 5 (resp. Fig. 6). One may notice that the resulting images (Fig. 5 and Fig. 6) are smaller than the original ones, because the technique for computing the values  $V_i(P)$  for each pixel  $P$  inside the sliding mask  $F(P)$  (see Eq. 2) provides no information inside the boards of the initial image, the width of the boards being equal to the radius of the sliding mask. The six classes are coloured with a red to green colour scale to show the progressive decreasing in the continuity of built up zones. On both maps the presence of parks in the south east of

the capital (in orange and in yellow) contrast with the downtown (bright orange) and the built up zones southward along the Seine which appears in the same category than southern suburbs where activity zones have been progressively concentrated from the fifties up to now. The map obtained with the smallest measuring mask (Fig. 5) shows more precisely (in red) the continuity of the built-up area around recent poles such as the southern airport and the main food market of the capital.

The whole processing has been equally applied on two SPOT sub scenes of the Oursi region in the Sahel (Burkina Faso) taken in August, during the wet season (Fig. 8) and in December after the wet season (Fig. 9) in order to quantify the inter seasonal dynamics of the vegetation cover in Sahel. Vegetation cover is first extracted by an automatic multispectral classification (Fig. 10 and Fig. 11). The differences  $\Delta v_i$  between the mean values of granulometric classes computed from the December and the August scenes is shown on Table 2.

One may notice from Table 2 that negative values for the  $\Delta v_i$ , which corresponds to higher values of  $v_i$  in August, are higher and more frequent for most of the classes. It means that the macro-texture of the vegetation cover is more heterogeneous in August than in December. In another hand, it may be observed by comparing the profiles of classes  $C_1$  and  $C_2$ , which contains the sets of biggest particles for both scenes, that the scene of December contains obviously more particles of median size (size 4) than the one of August.

Table 1. *Mean values of the granulometric density  $v_i$  for each class obtained by the k-Means method from the binary image of the Paris region on Fig. 3 analysed with a circular structuring element inside a 200-pixels-wide circular measuring mask.*

	$v_1$	$v_2$	$v_3$	$v_4$	$v_5$	$v_6$	$v_7$	$v_8$	$v_9$	$v_{10}$
$C_1$	44	58	33	49	62	88	90	116	102	135
$C_2$	56	97	101	104	79	91	48	29	23	1
$C_3$	86	135	112	85	31	5	7	1	1	0
$C_4$	136	107	87	28	14	7	3	2	3	0
$C_5$	151	153	38	11	1	2	1	1	0	0
$C_6$	213	71	10	1	1	0	0	0	0	0

Table 2. *Difference  $\Delta v_i$  between mean values of the granulometric density  $v_i$  of the binary images of Oursi region from the Spot scenes of August and December 1986.*

	$\Delta v_1$	$\Delta v_2$	$\Delta v_3$	$\Delta v_4$	$\Delta v_5$	$\Delta v_6$	$\Delta v_7$	$\Delta v_8$	$\Delta v_9$
$C_1$	16	7	36	34	-85	19	-104	0	0
$C_2$	-5	-21	-11	45	-81	-8	-1	0	0
$C_3$	0	5	-60	-4	11	-3	-1	0	0
$C_4$	-19	-40	35	8	2	0	0	0	0
$C_5$	-25	5	16	-2	0	0	0	0	0
$C_6$	-21	20	7	-2	0	0	0	0	0

Comparison between both granulometric maps shows that herbaceous vegetation rapidly invades large topographic depressions in the south east of the scene during the raining season (Fig. 12). Two months after the rainfalls (Fig. 13), ligneous vegetation still colonise small depressions on the northern sand dunes and has yet markedly invaded the main north-south oriented channels, as the continuous herbaceous cover has already vanished.

Although there is not a clear correspondence between granulometric classes of macro texture

between the two periods, granulometric maps shows that the process of contraction of ligneous cover depends both on climatic and on topographic conditions: For a given amount of rainfall during the wet season, ligneous vegetation will colonise topographic depressions all during the first part of the dry season. If there is a deficit in raining water for a long period in arid zones, the contraction of vegetation may increase, which may be detected by analysing the change of granulometric classes between images taken at two different years during the dry season.



Fig. 8. SPOT scene on the Oursi region (August 1986).

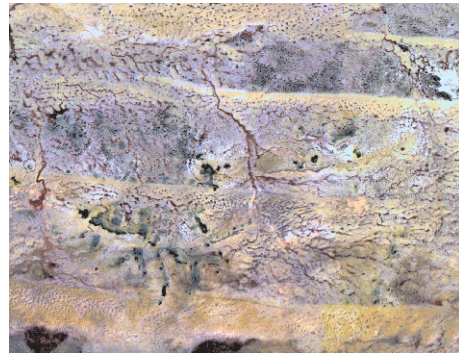


Fig. 9. SPOT scene on the Oursi region (December 1986).

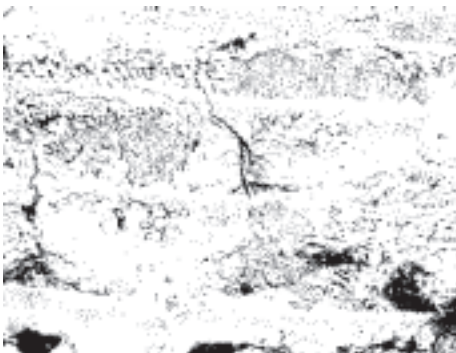


Fig. 10. Vegetation cover in the Oursi region during the wet season.

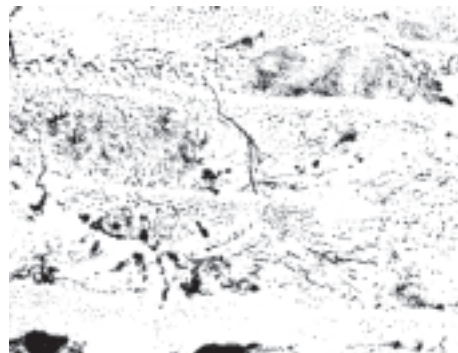


Fig. 11. Ligneous cover in the Oursi region after the wet season.

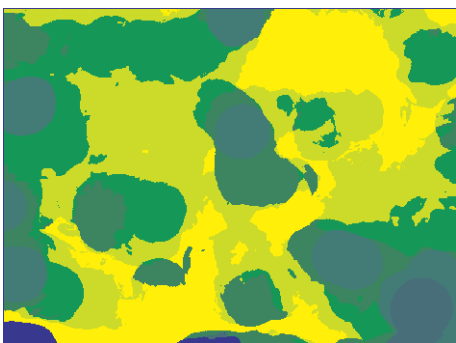


Fig. 12. Granulometric map of the vegetation cover in Oursi during the wet season.

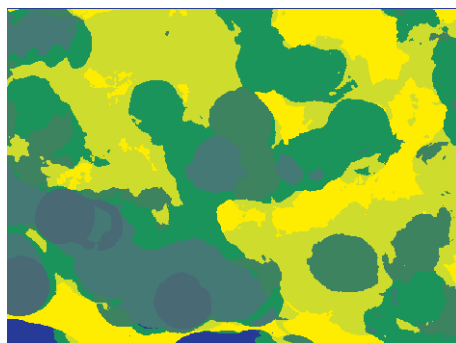


Fig. 13. Granulometric map of the ligneous cover in Oursi after the wet season.

## REFERENCES

- Aubert A, Jeulin D, Hashimoto R (2000). Surface texture classification from Morphological transformations. ISMM 2000, Palo Alto, 26-28 juin 2000.
- Borgefors G (1986). Distance transformations in digital images. CGIP 34:344-71.
- Danielsson PE (1980). Euclidian distance mapping. CGIP 14:227-48.
- Diday E (1974). Classification Automatique Séquentielle pour Grands Tableaux. Rev. Fr. Rech. Opér. 9ème année, (Mars 1975), 1-29.
- Harralick RM (1978). Statistical and structural approaches to texture. Proceedings IEEE, Dept of Computer Science. University of Kansas, 67:786-804.
- Matheron G (1975). Random Sets and Integral Geometry. New York: Wiley and sons.
- Mering C, Callot Y, Kemmouche A (1997). Analysis and Mapping of natural landscapes from satellite images using Morphological Filters. Microsc Microanal Microstruct 7:323-30.
- Serra J (1982). Image Analysis and Mathematical Morphology. London: Academic Press.